Article

Discovery Medicine 2025; 37(196): 946–956
https://doi.org/10.24976/Discov.Med.202537196.84

Investigating Anti-Tumor Effects of Irisin in Cervical Cancer Cells: Cell Viability, Migration, and Tumor-Associated Macrophage Polarization

Guanyu Cao[1], Yan Wei[1], Xiaojie Ma[1,*]

[1]Department of Gynaecology, Tongxiang First People's Hospital, 314500 Tongxiang, Zhejiang, China
*Correspondence: maxiaojie7753@163.com (Xiaojie Ma)
Published: 20 May 2025

Background: Cervical cancer is a major concern in women's health. Investigating the biological behavior of cancer cells can help to understand the underlying pathogenesis and offer novel insights into disease management. Therefore, this study evaluated the effect of irisin on the biological behaviors of cervical cancer cells and elucidated its underlying mechanism.
Methods: Cell viability of Caski and HeLa cells under different irisin concentrations was examined using the cell counting kit-8 (CCK-8) assay. Cell proliferation and autophagy levels were assessed at protein and mRNA levels using Western blot (WB) and quantitative real-time polymerase chain reaction (qRT-PCR) analyses, respectively. Apoptosis was determined by assessing the levels of activated caspase-3, caspase-8, and caspase-9 using corresponding enzyme-linked immunosorbent assay (ELISA) kits. The impact of irisin on cell cycle and apoptosis rates was evaluated using flow cytometry analysis. However, the migratory capability of irisin-treated cells was assessed using the scratch healing assay. Furthermore, expression levels of matrix metalloproteinases (MMP2, MMP7, and MMP9) were determined using WB analysis, and the Transwell assay assessed the invasive potential of the cells. The impact of irisin on macrophage polarization was examined through CD86 and CD206 typing using flow cytometry, and macrophage polarization status was determined by detecting the levels of inflammatory cytokines (interleukin (IL)-6, IL-10) and tumor necrosis factor-α (TNF-α). Then, THP-1 cells were directly co-cultured with cervical cancer cells to detect their effect on their biological behavior with or without irisin treatment, aiming to explore the underlying mechanism.
Results: Irisin reduces cervical cancer cell viability and decreases the protein and mRNA expression levels of minichromosome maintenance complex component 2 (MCM2), antigen identified by monoclonal antibody Ki67 (Ki67), and proliferating cell nuclear antigen (PCNA) ($p < 0.05$) in a dose-dependent manner, resulting in G0/G1 cell cycle arrest ($p < 0.05$). Irisin suppresses the expression of autophagy-related proteins Beclin-1 and microtubule-associated protein 1 light chain 3 (LC3) ($p < 0.05$), increases the content of cleaved caspase-3, cleaved caspase-8, and cleaved caspase-9 ($p < 0.05$), and enhances the apoptosis rate ($p < 0.05$). Additionally, irisin suppresses cervical cancer cell migration and reduces the expression of MMP2, MMP7, and MMP9 proteins ($p < 0.05$). Furthermore, it increases the number of CD86-positive cells ($p < 0.05$) while increasing the content of M1-type cytokine IL-6 and TNF-α ($p < 0.05$) and reducing the levels of M2-type cytokines IL-10 ($p < 0.05$), thereby promoting M1 polarization. The altered polarization state affects the apoptosis rate ($p < 0.05$), invasiveness ($p < 0.05$), and autophagy levels ($p < 0.05$) of cervical cancer cells in co-cultures with macrophages.
Conclusion: Irisin exhibits potent anti-cancer effects on cervical cancer cells by modulating several key cellular processes and altering the tumor microenvironment. Irisin effectively inhibits the proliferation, invasion, and migration of cervical cancer cells and affects the levels of autophagy and apoptosis. Furthermore, it inhibits cancer cells by affecting the polarization of tumor-associated macrophages, underscoring their potential as a novel therapeutic target for treating cervical cancer.

Keywords: cervical cancer; irisin; biological behavior; macrophage; polarization

Introduction

Cervical cancer is one of the most prevalent malignant tumors in women globally, with particularly high incidence and mortality rates in developing countries [1]. Cellular proliferation is fundamental to the development of cervical cancer. Additionally, invasive and migratory capabilities are crucial to malignant behavior [2]. Various cytokines, such as interleukins (IL-6, IL-10), tumor necrosis factor-α (TNF-α), and matrix metalloproteinases (MMPs), play vital roles in these invasion and migration processes [3]. These biological behaviors underline the metastasis of cervical cancer significantly impact its progression and prognosis. Therefore, understanding the underlying biological mechanisms is essential for developing new diagnostic approaches and therapeutic strategies.

Irisin, first identified in 2012 by Professor Bruce Spiegelman's research team [4], is a peptide hormone en-

coded by the fibronectin type III domain-containing protein 5 (*FNDC5*) gene and secreted by muscle cells after physical exercise. It is a cleaved and glycosylated fragment derived from the C-terminal region of the FNDC5 protein, typically comprising about 112 amino acid residues [5]. Initially recognized for its expression in muscle cells and its exercise-related physiological effects, subsequent research has revealed its roles in various physiological processes. Recent studies have shown that irisin plays significant roles in various cancer types, especially in modulating tumor cell proliferation, invasion, and migration [6]. For instance, irisin has been reported to inhibit the phosphatidylinositol 3-kinase (PI3K)/protein kinase B (AKT) pathway, ultimately suppressing proliferation, migration, and invasion of lung cancer cells and downregulating the expression of epithelial-mesenchymal transition (EMT) markers [7]. On the contrary, a study by Celik *et al*. [8] observed substantially lower serum irisin levels in colorectal cancer patients than in the control group. On the other hand, increased irisin levels have been reported in hepatocellular carcinoma, improving the proliferation, migration, and invasion of HepG2 and SMMC7721 cells [9]. Furthermore, irisin has been proposed to mediate crosstalk between hepatic stellate cells and macrophages [10]. Despite these advancements, the specific mechanisms underlying irisin's effects in cervical cancer remain largely unexplored.

The tumor microenvironment (TME) is a highly dynamic and complex ecosystem composed of tumor cells, immune cells, fibroblasts, vascular endothelial cells, extracellular matrix, and various soluble factors [11]. Among the immune cells, macrophages play a critical role, with their polarization state closely affecting the proliferation, migration, and invasion of cancer cells [12]. Within the TME, macrophages are typically polarized toward the M2-type, which contributes to immunosuppression by secreting IL-10, thereby suppressing T cell activity and reducing overall immune responses [13]. Furthermore, M2-type macrophages degrade the extracellular matrix by secreting MMPs, facilitating invasion and metastasis of tumour cells [14]. On the contrary, M1-type macrophages exert anti-tumor activity. They secrete pro-inflammatory cytokines such as TNF-α, IL-1β, and IL-6, which directly target tumor cells and activate adaptive immune responses by enhancing T cell-mediated anti-tumor immune responses [15]. Furthermore, M1-type macrophages produce reactive oxygen species (ROS) and nitric oxide (NO), enhancing local inflammatory response and inhibiting the growth and dissemination of tumor cells [16]. Research revealed that inhibiting M2-type macrophage polarization substantially suppressed lung cancer metastasis and progression [17], highlighting the therapeutic potential of macrophage polarization in cancer management.

This study aims to investigate the effects of irisin on the biological behavior of cervical cancer cells and to uncover its potential molecular mechanisms. Particularly, it intends to assess whether irisin can influence key cellular processes such as proliferation, migration, and invasion. Additionally, the study will explore the impact of irisin on adjacent macrophages to identify novel therapeutic targets and strategies for treating cervical cancer.

Materials and Methods

Cell Culture

Cervical cancer cell lines, including HeLa (CCL-2), CaSki (CRL-1550), and THP-1 cells (TIB-202), were purchased from American Type Culture Collection (ATCC; Manassas, VA, USA). The cells were cultured in Dulbecco's modified eagle medium (11320033, DMEM, Gibco, Shanghai, China) supplemented with 10% fetal bovine serum (A5256701, FBS, Gibco, Shanghai, China), 1$\times$ penicillin, and streptomycin (PB180120, Procell, Wuhan, China) at 37 °C with 5% CO_2 for 24 hours. The cells were authenticated using short tandem repeat (STR) analysis, while mycoplasma testing confirmed the absence of mycoplasma contamination. Cells grown to about 80% confluency were trypsinized. After centrifugation at 1000 rpm for 5 minutes, the cells were resuspended in fresh medium and inoculated into cell plates at the appropriate ratio.

Cell Counting Kit-8 (CCK-8)

The cervical cancer cell suspension, containing about 10,000 cells, was inoculated into 96-well plates and incubated for 24 hours to allow proper cell adherence to the wall. Then, the cells were treated with different concentrations of irisin (5 nmol/L, 10 nmol/L, 20 nmol/L, and 50 nmol/L; SRP8039, Merck, Shanghai, China) for 24, 48, and 72 hours. After treatment, 10 µL of CCK-8 solution (CK04, Dojindo, Kumamoto, Japan) was added to each well containing 100 µL of the medium, and the culture plates were incubated for 2 hours. Absorbance was measured at 450 nm using a microplate reader (ELX800, BioTek Instruments, Inc., Winooski, VT, USA). Cell viability was calculated employing the following formula: Cell viability (%) = (Absorbance of the experimental group – Absorbance of blank) / (Absorbance of the control group – Absorbance of blank) $\times$ 100%.

Western Blot (WB) Analysis

Treated cells were lysed on ice using radio immunoprecipitation assay (RIPA) buffer (P0013B, Beyotime, Shanghai, China) to obtain total protein. Protein concentration was determined using the bicinchoninic acid assay (BCA, 23227, ThermoFisher Scientific, Inc., Waltham, MA, USA). Equal amounts of protein were resolved using Sodium Dodecyl Sulfate (SDS)-polyacrylamide gel electrophoresis and were transferred onto polyvinylidene fluoride (PVDF) membranes (FFP39, Beyotime, Shanghai, China). The membranes underwent overnight incu-

bation at 4 °C with primary antibodies targeting specific proteins. The following day, membranes were washed with tris-buffered saline containing tween-20 (TBST) to remove unbound primary antibodies. Horseradish peroxidase (HRP)-labeled secondary antibodies, such as anti-mouse immunoglobulin G (IgG) (1:2000; 12-349, Merck, Shanghai, China) and anti-rabbit IgG (1:2000; 12-348, Merck, Shanghai, China) corresponding to the primary antibody were then applied and incubated at room temperature for 1 hour. Grey values of protein bands were assessed using ImageJ (version 5.0; Bio-Rad, Hercules, CA, USA).

The antibodies and their dilutions used in the study included: proliferating cell nuclear antigen (PCNA) (1:1500, cat.ab29, Abcam, Shanghai, China), minichromosome maintenance complex component 2 (MCM2) (1:1500, cat.ab4461, Abcam), antigen identified by monoclonal antibody Ki67 (Ki67) (1:1500, cat.ab15580, Abcam), MMP2 (1:1000, cat.10373-2-AP, Proteintech, Wuhan, China), MMP7 (1:1500, cat.10374-2-AP, Proteintech), MMP9 (1:1000, cat.10375-2-AP, Proteintech), Beclin-1 (1:1000, cat.3738, Cell Signaling Technology, Danvers, MA, USA), microtubule-associated protein 1 light chain 3 (LC3) (1:1000, cat.2775, Cell Signaling Technology), and β-actin (1:2000, cat. ab8226, Abcam).

RNA Isolation and Quantitative Real-Time Polymerase Chain Reaction (qRT-PCR)

Total RNA from cells was extracted using TRIzol reagent (15596026CN, Invitrogen, Thermo Fisher Scientific, Inc., Waltham, MA, USA). After examining the purity, RNA was reverse-transcribed into complementary DNA (cDNA). The expression levels of target genes were determined using qRT-PCR (Applied Biosystems StepOne Plus system, Applied Biosystems, Foster City, CA, USA), with glyceraldehyde 3-phosphate dehydrogenase (GAPDH) serving as an internal reference. The average CT value of three replicate wells was calculated for each cell group. The expression levels of target genes were determined using the $2^{-\Delta\Delta CT}$ method, and the fold change relative to the control group was calculated.

The primer sequences used in qRT-PCR are listed below: *PCNA* Forward: 5′-GCCCTGGTTCTGGAGGTAAC-3′; Reverse: 5′-CATCCTCGATCTTGGGAGCC-3′. *Ki67* Forward: 5′-CTGACCCTGATGAGAGTGAGGGA-3′; Reverse: 5′-ACTCTGTAGGGTCGAGCAGG-3′. *MCM2* Forward 5′-CTACCAGCGTATCCGAATCCA-3′; Reverse 5′-CCTACAGCAACCTTGTTGTCCT-3′. *LC3* Forward 5′-TTCAGGTTCACAAAACCCGC-3′; Reverse 5′-GACACTGGTACACTGCTGCT-3′. *Beclin-1* Forward 5′-GGTTGCGGTTTTTCTGGGAC-3′; Reverse 5′-GAGCAGAGTCGGCATTCAGT-3′. *GAPDH* Forward: 5′-TCATGGGTGTGAACCATGAGAA-3′; Reverse 5′-GGCATGGACTGTGGTCATGAG-3′.

Enzyme-Linked Immunosorbent Assay (ELISA)

The ELISA kits were used to assess the cellular levels of IL-6 (cat. SEKH-0014, Solarbio, Beijing, China), TNF-α (cat. SEKH-0047, Solarbio), IL-10 (cat. SEKH-0018, Solarbio), caspase-3 cleaved (cat. KHO1091, Thermo Fisher Scientific, Invitrogen, USA), caspase-8 cleaved (cat. CBC1003, Assay Biotechnology, SAN Jose, CA, USA), and caspase-9 cleaved (cat. KL-4217Hu, Kanglang, Shanghai, China), following the manufacturer's instructions. Briefly, cell culture supernatants or lysates and standards of known concentrations were incubated with the enzyme-labeled antibody working solution at room temperature for one hour. After thorough washing, a colorimetric substrate was added and incubated for 30 minutes at room temperature. After another wash, the reaction was terminated using a termination solution, and absorbance was measured at 450 nm using a microplate reader (ELX800, BioTek Instruments, Inc., Winooski, VT, USA). Finally, the concentrations of target proteins were calculated based on the standard curves.

Flow Cytometry

Cells in the log growth phase were collected, adjusted to a density of 1×10^6/mL, and washed with phosphate buffered saline (PBS). For apoptosis analysis, cells were incubated with 5 µL of membrane-bound protein V-FITC and 10 µL of propidium iodide (PI) working solution for 15 minutes at room temperature in the dark, using the Annexin V/PI double staining kit (cat.556547, BD Biosciences, San Jose, CA, USA). For cell cycle analysis, cells were fixed in 70% ethanol at 4 °C for 24 hours. After washing, they were treated with ribonuclease (RNase) at 0.5 mg/mL for 30 minutes at 37 °C, followed by staining with propidium iodide (PI, 50 µg/mL) for 30 minutes at 4 °C in the dark. For CD86 and CD206 phenotyping [18], cells were fixed, permeabilized, and incubated with FITC-coupled anti-human CD86 (11-0862-82) and BV421-coupled anti-human CD206 (48-2069-42) (eBioscience, San Diego, CA, USA) antibodies. Finally, the stained cells were analyzed using BD LSR II flow cytometry.

Scratch Healing Assay

Cell suspensions containing about 10,000 cells were inoculated into 96-well plates and incubated for 24 hours until achieving approximately 80% confluency. To reduce the effect of cell proliferation on the results, cells were starved using a serum-free medium for an additional 24 hours. A straight-line scratch was created over the cell monolayer using a 200 µL pipette. The cell surface was gently rinsed with PBS to remove detached cells, ensuring clean and uniform wound edges. After the drug treatment, cells were incubated for 24 hours, and the wound was photographed using an inverted microscope (TS100, Nikon, Tokyo, Japan) to assess cell migration. The wound healing

rate was determined using the following formula: Wound healing rate (%) = (Initial wound width – Current wound width)/Initial wound width × 100%.

Transwell

Cell suspensions containing approximately 2×10^5 cells were inoculated into 24-well plates (cat.3524, Corning, Shanghai, China) and incubated until reaching about 80% confluency. The cells were then starved using a serum-free medium for 24 hours. The upper layer of the Transwell chambers was coated with matrix gel (Matrigel), while the lower chamber was filled with serum-containing medium serving as a chemoattractant. Treated cell suspension was added to the upper chamber and incubated for 24 hours. Cells were then fixed with 4% paraformaldehyde for 15 minutes and stained using crystal violet (C0121, Beyotime, Shanghai, China). Cells migrated to the lower chambers were photographed using an inverted microscope. For quantification, cells were counted in 5 randomly selected fields per chamber, and the average migrated cells was calculated.

Macrophages Co-Cultured With Cervical Cancer Cells

HeLa or Caski, and THP-1 cells were cultured separately in the medium for 24 hours until achieving about 70–80% confluence. THP-1 cells were inoculated into 6-well plates at a density of 5×10^5/mL, and then treated with (Phorbol Myristate Acetate (PMA) 50 ng/mL, P1585, Sigma, St Louis, MO, USA) for 16 hours to induce differentiation into M0-type macrophages [19]. After removing the old medium from the cervical cancer cell cultures, the PMA-treated THP-1 cells were inoculated into 6-well plates along with cervical cancer cells at a 1:1 ratio. The co-cultured cells were incubated for 48 hours, followed by treatment with 10 nmol/L irisin for 48 hours.

Statistical Analysis

Statistical analyses were performed using GraphPad Prism version 7.0 (GraphPad Software Inc., San Diego, CA, USA). Experimental data were expressed as mean ± standard deviation (SD), and statistical differences between groups were assessed using one-way Analysis of Variance (ANOVA) followed by Bonferroni post hoc tests. Each experiment was conducted in triplicate. *, **, *** denote significance at $p < 0.05$, $p < 0.01$, $p < 0.001$, respectively. A $p < 0.05$ indicated a statistically significant difference.

Results

Irisin Inhibits the Proliferation of Cervical Cancer Cells

Cervical cancer cells (Caski and HeLa) were treated with different concentrations of irisin for varying periods. As shown in Fig. 1a,b, cell viability in both Caski and HeLa cells significantly decreased in a concentration-dependent manner after irisin treatment ($p < 0.05$). Notably, a highly significant reduction in cell viability was found after 48 hours of exposure to 10 nmol/L irisin [20], which was chosen as the optimal conditions for subsequent experiments.

Furthermore, to assess the expression levels of proliferation markers, WB and RT-PCR analyses were performed. The results showed that irisin significantly reduced the expression levels of Ki67, MCM2, and PCNA in a dose-dependent manner ($p < 0.05$, Fig. 1c–i). Moreover, flow cytometry was used to examine cell cycle distribution. Analysis revealed that increasing irisin concentrations led to a significant accumulation of cells in the G0/G1 phase ($p < 0.05$), indicating that irisin causes cell cycle arrest at the G0/G1 phase, thereby inhibiting the proliferation of cervical cancer cells (Fig. 1j,k).

Irisin Inhibits Autophagy and Promotes Apoptosis in Cervical Cancer Cells

While irisin effectively inhibits the proliferation of cervical cancer cells, its effects on cellular autophagy and apoptosis were assessed in subsequent experiments. The protein and mRNA expression levels of autophagy-related markers Beclin-1 and LC3 were evaluated (Fig. 2a–e), demonstrating that irisin significantly suppresses autophagy in cervical cancer cells ($p < 0.05$). Furthermore, the levels of cleaved caspase-3, cleaved caspase-8, and cleaved caspase-9 in the cell lysate were assessed (Fig. 2f–h), revealing that irisin significantly elevates apoptosis ($p < 0.05$). Additionally, the apoptosis rate was measured using flow cytometry analysis, revealing that 10 nmol/L irisin significantly induced apoptosis in both Caski and HeLa cells ($p < 0.05$, Fig. 2i–k).

Collectively, these findings demonstrate that irisin inhibits protective autophagy while promoting apoptosis in cervical cancer cells.

Irisin Inhibits Migration and Invasion of Cervical Cancer Cells

Migration and invasion are fundamental processes underlying the distant metastasis of cancer cells. Therefore, in subsequent experiments, we investigated the effects of irisin on the migration and invasion of cervical cancer cells. The scratch wound healing assay was used to assess cellular migration. As shown in Fig. 3a,b, irisin reduced wound closure rate in a dose-dependent manner, indicating that irisin significantly inhibits the migratory capability of cervical cancer cells ($p < 0.05$). MMPs, especially MMP2, MMP7, and MMP9, promote cell proliferation, migration, and invasion, and are widely used as biomarkers for the invasive or migratory potential of cervical cancer cells. Western blot analysis demonstrated that the expression levels of MMP2, MMP7, and MMP9 were substantially reduced after irisin treatment compared to the control group ($p < 0.05$, Fig. 3c–

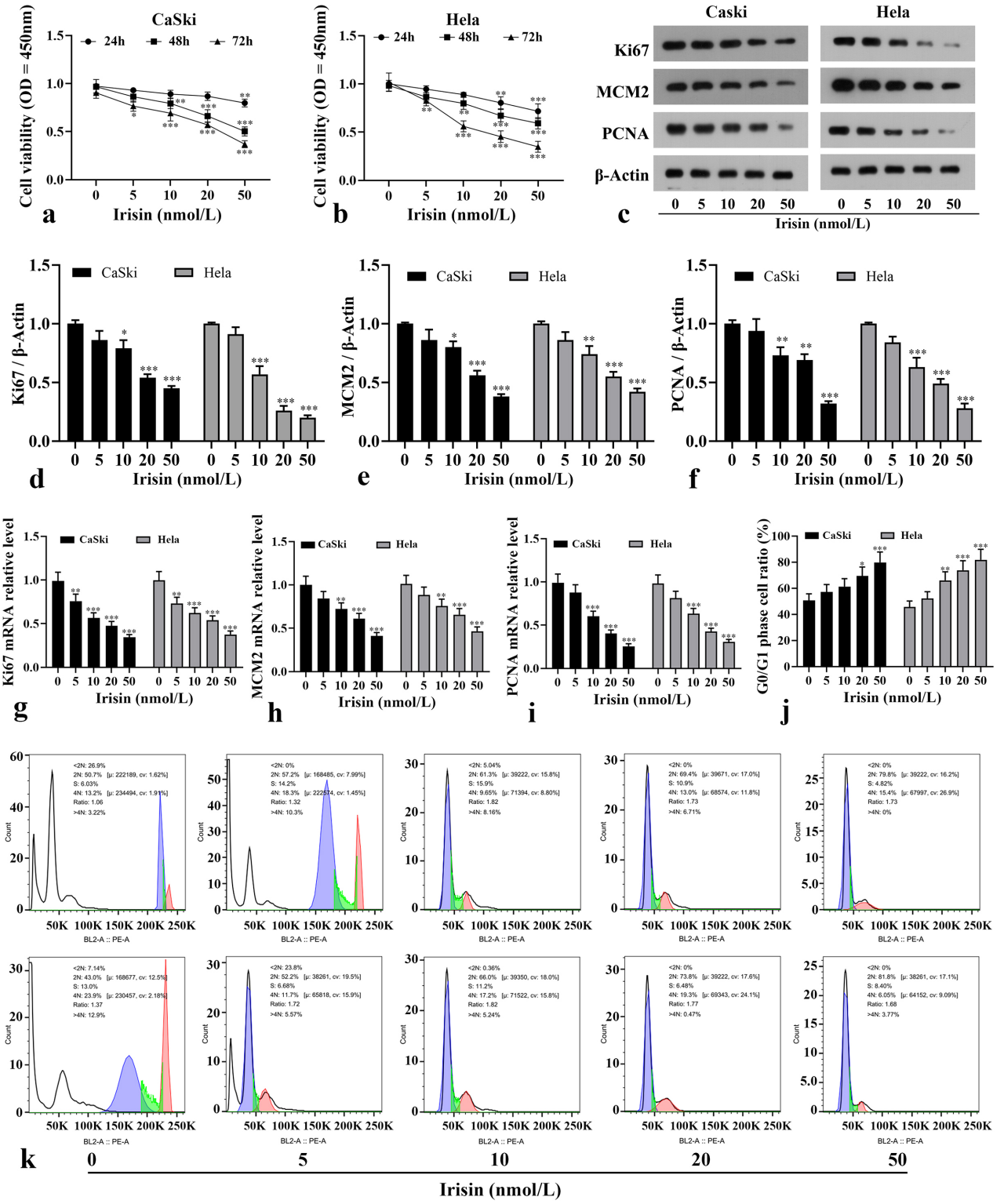

Fig. 1. Irisin inhibits the proliferation of cervical cancer cells. (a,b) CCK-8 assay was used to evaluate cell activity (n = 6). (c–f) Irisin reduces the protein levels of Ki67, MCM2, and PCNA (n = 3). (g–i) Irisin reduces the mRNA levels of Ki67, MCM2, and PCNA (n = 6). (j,k) Flow cytometry was used to evaluate cell cycle (n = 3). *$p < 0.05$, **$p < 0.01$, ***$p < 0.001$, compared to the 0-concentration treatment in the same group. OD, Optical Density; CCK-8, cell counting kit-8; MCM2, minichromosome maintenance complex component 2; PCNA, proliferating cell nuclear antigen; Ki67, antigen identified by monoclonal antibody Ki67.

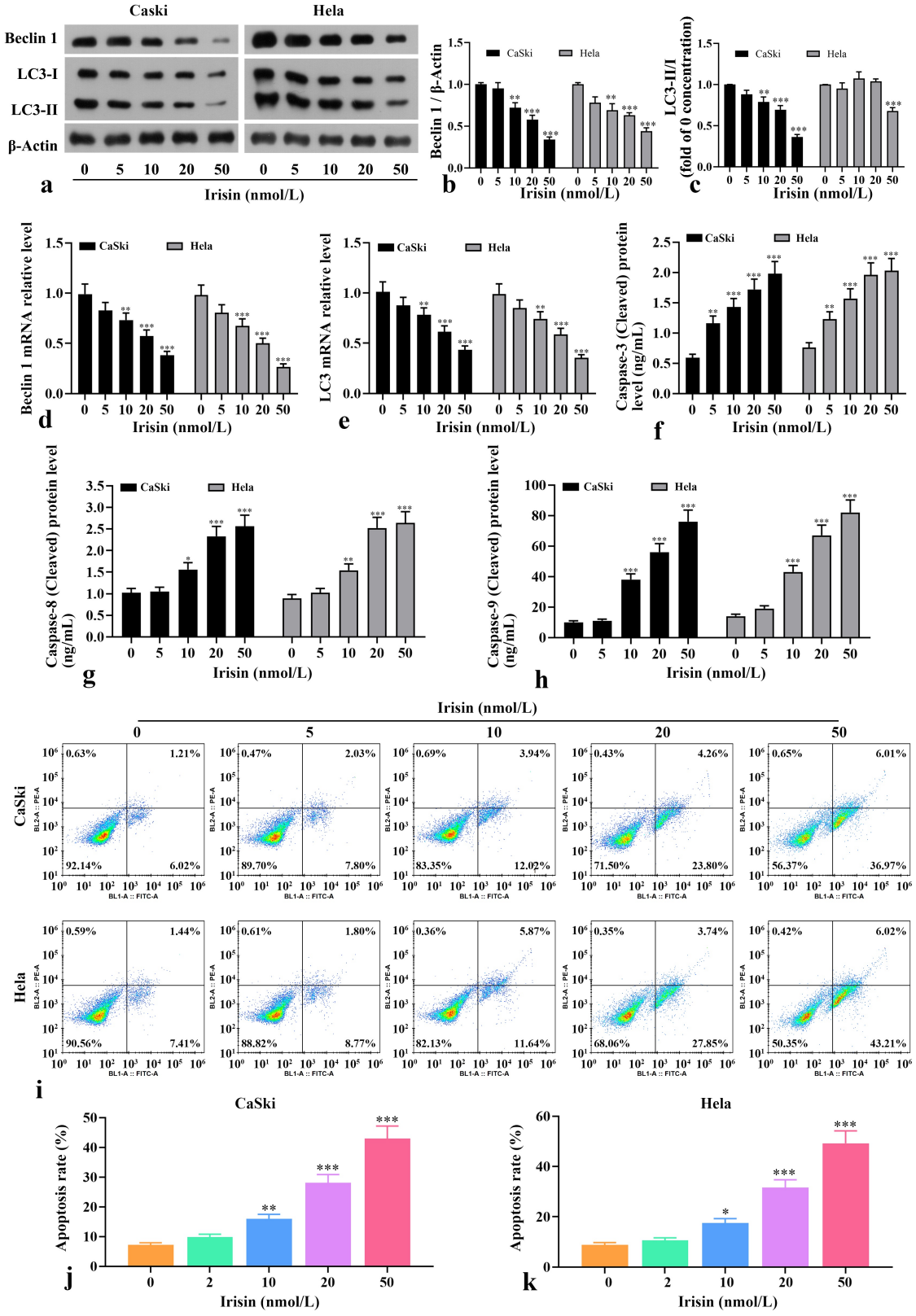

Fig. 2. Irisin inhibits autophagy and promotes apoptosis in cervical cancer cells. (a–c) Irisin reduces levels of the autophagy-related proteins Beclin and LC3 (n = 3). (d,e) Irisin reduces mRNA levels of autophagy-related proteins Beclin 1 and LC3 (n = 6). (f–h) ELISA was used to assess the levels of cellular cleaved caspase-3, cleaved caspase-8, and cleaved caspase-9 (n = 3). (i–k) Flow cytometry was applied to assess the apoptosis (n = 3). *$p < 0.05$, **$p < 0.01$, ***$p < 0.001$, compared to the 0-concentration treatment in the same group. LC3, microtubule-associated protein 1 light chain 3; ELISA, enzyme-linked immunosorbent assay.

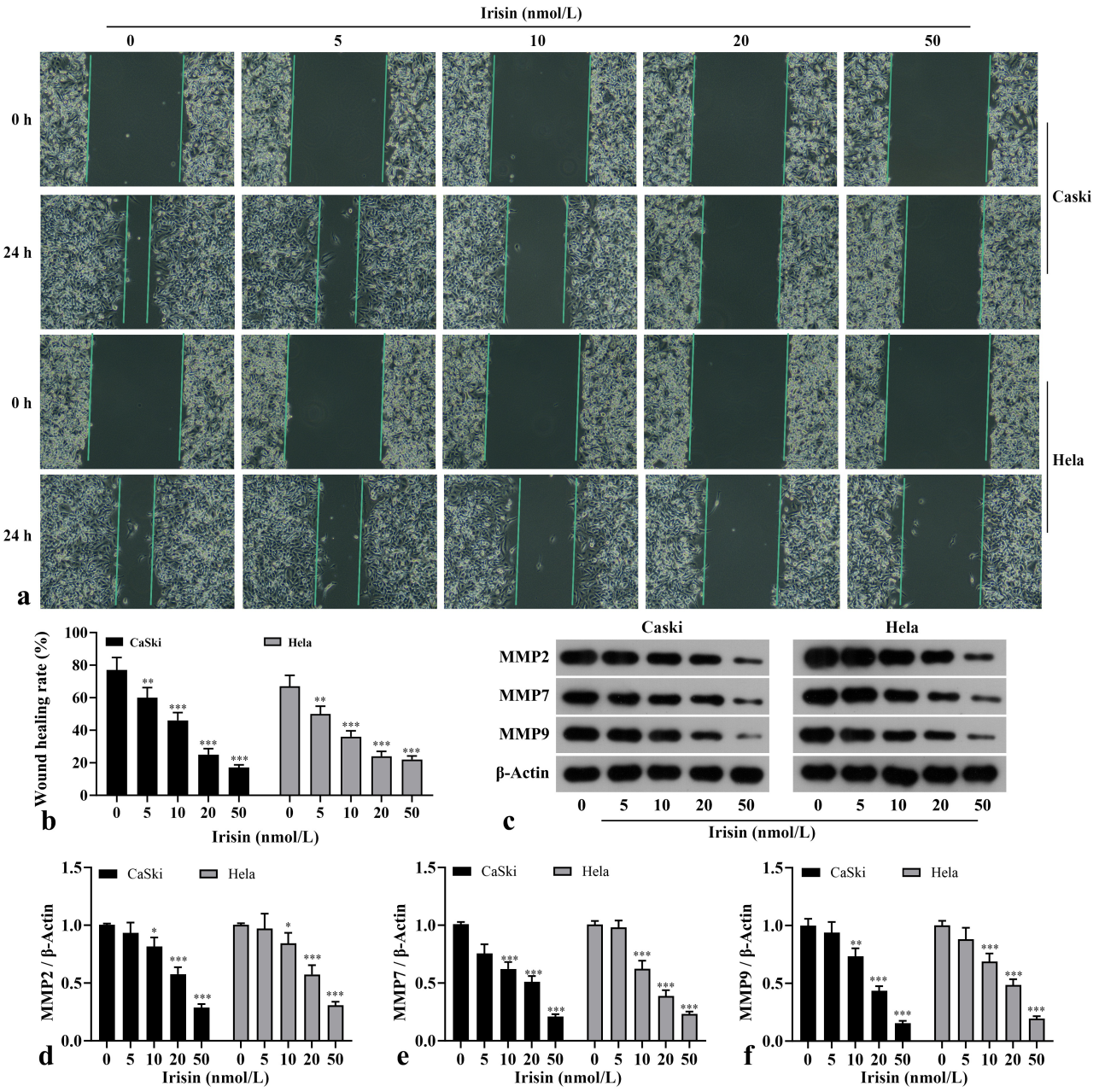

Fig. 3. Irisin inhibits cervical cancer cell migration and invasion. (a,b) The scratch healing assay was used to assess cell migration (n = 3). (c–f) WB analysis was used to determine the levels of MMP2, MMP7, and MMP9 (n = 3). *$p < 0.05$, **$p < 0.01$, ***$p < 0.001$, compared to the 0-concentration treatment in the same group. WB, Western blot; MMP2, matrix metalloproteinase-2.

f). These observations confirm that irisin significantly inhibits the migratory or invasive capabilities of cervical cancer cells.

Irisin Promotes M1 Polarization of Tumor-Associated Macrophages

During cancer development, changes in the tumor micro-environment, comprising various surrounding cells, play a crucial role in tumor initiation, progression, metastasis, and therapeutic response. Given the key role of macrophages in the tumor micro-environment, we focused on the effects of irisin on tumor-associated macrophages. As shown in Fig. 4a, THP-1 cell viability decreased with increasing concentrations of irisin ($p < 0.05$), with a significant inhibitory effect observed at 10 nmol/L irisin after 48 hours of treatment. Subsequently, two experimental groups were established: the THP-1 cell and the THP-1 cell + irisin group (treated with 10 nmol/L irisin). Flow cytometry analysis assessed THP-1 cell phenotype (Fig. 4b–d). The results show a substantial increase in CD86-positive cells (*p*

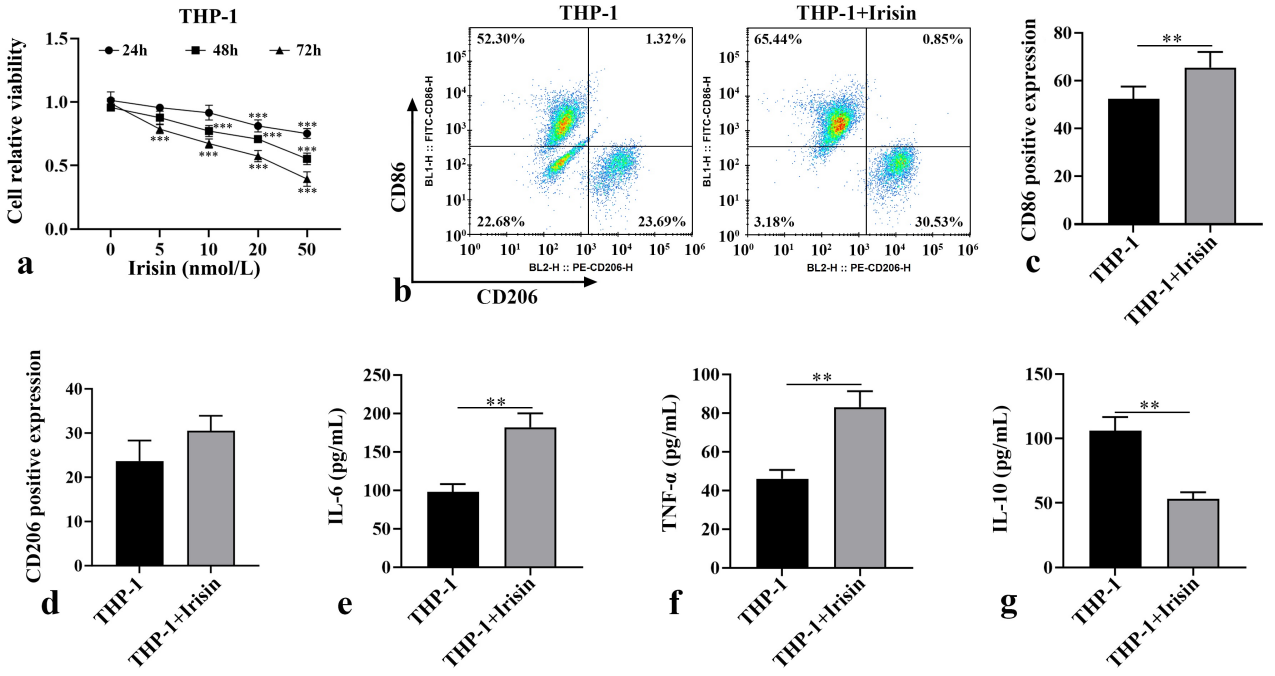

Fig. 4. Effect of irisin on the polarization of tumor-associated macrophages. (a) CCK-8 assessment of THP-1 cell activity (n = 6). (b) Flow cytometry analysis of cell surface antigen CD86 and CD206 expression (n = 3). (c) Macrophage surface antigen CD86 expression (n = 3). (d) Macrophage surface antigen CD206 expression (n = 3). (e–g) Levels of inflammatory cytokines IL-6, TNF-α, and IL-10 were assessed using ELISA (n = 3). $^{**}p < 0.01$, $^{***}p < 0.001$, compared to the 0-concentration treatment in the same group. IL, interleukin; TNF-α, tumor necrosis factor-α.

< 0.05) and no significant change in CD206-positive cells ($p > 0.05$) after irisin treatment, indicating a shift toward the CD86 phenotype. These results suggest that irisin promotes M1-type polarization of THP-1-derived macrophages.

To further confirm the polarization phenotype, we measured cytokine levels in the culture supernatants of these two groups. As shown in Fig. 4e–g, irisin treatment significantly decreased the levels of the anti-inflammatory cytokine IL-10 and increased the levels of the pro-inflammatory cytokines IL-6 and TNF-α ($p < 0.05$). These results confirm that irisin promotes M1 polarization of THP-1 cells.

Irisin Regulates Macrophage Polarization to Inhibit Cervical Cancer Cells

As we observed that irisin promotes M1 polarization of macrophages, therefore, to explored whether this shift in polarization impacts the migratory and invasive behaviors of cervical cancer cells, we co-cultured THP-1 cells with cervical cancer cells and treated the co-culture with 10 nmol/L irisin. Flow cytometry analysis revealed that co-culture with THP-1 cells substantially decreased the apoptosis rate of cervical cancer cells ($p < 0.05$). However, irisin treatment reversed this effect, significantly increasing the apoptosis rate ($p < 0.05$, Fig. 5a–c).

The invasive capacity of cervical cancer cells was assessed using a Transwell assay. As shown in Fig. 5d–f, the co-culture group increased the number of cervical cancer cells penetrating the Matrigel ($p < 0.05$), demonstrating enhanced invasive capacity. However, treatment with irisin significantly reduced the number of invading cervical cancer cells ($p < 0.05$), indicating a suppression of invasive capacity.

Additionally, we examined the protein and mRNA expression levels of the autophagy-related proteins Beclin-1 and LC3 (Fig. 5g–m). As expected, co-culture with THP-1 cells enhanced the autophagy levels in cervical cancer cells ($p < 0.05$), while irisin treatment significantly decreased the autophagy level ($p < 0.05$). These results demonstrate that irisin modulates macrophage polarization, which alters the proliferation and invasive capacity of cervical cancer cells.

Discussion

Cervical cancer is a major concern in women's health and remains a focus in medical research and treatment efforts [21]. In recent years, irisin has shown promising effects across various cancer types. Research has reported decreased serum irisin levels in breast cancer patients and has indicated that irisin inhibits the EMT process in cancer cells [22]. We observed similar experimental results. In this study, irisin significantly inhibited the proliferation of cervical cancer cells. Cell proliferation assays showed a significant decrease in the growth rate of cervical cancer

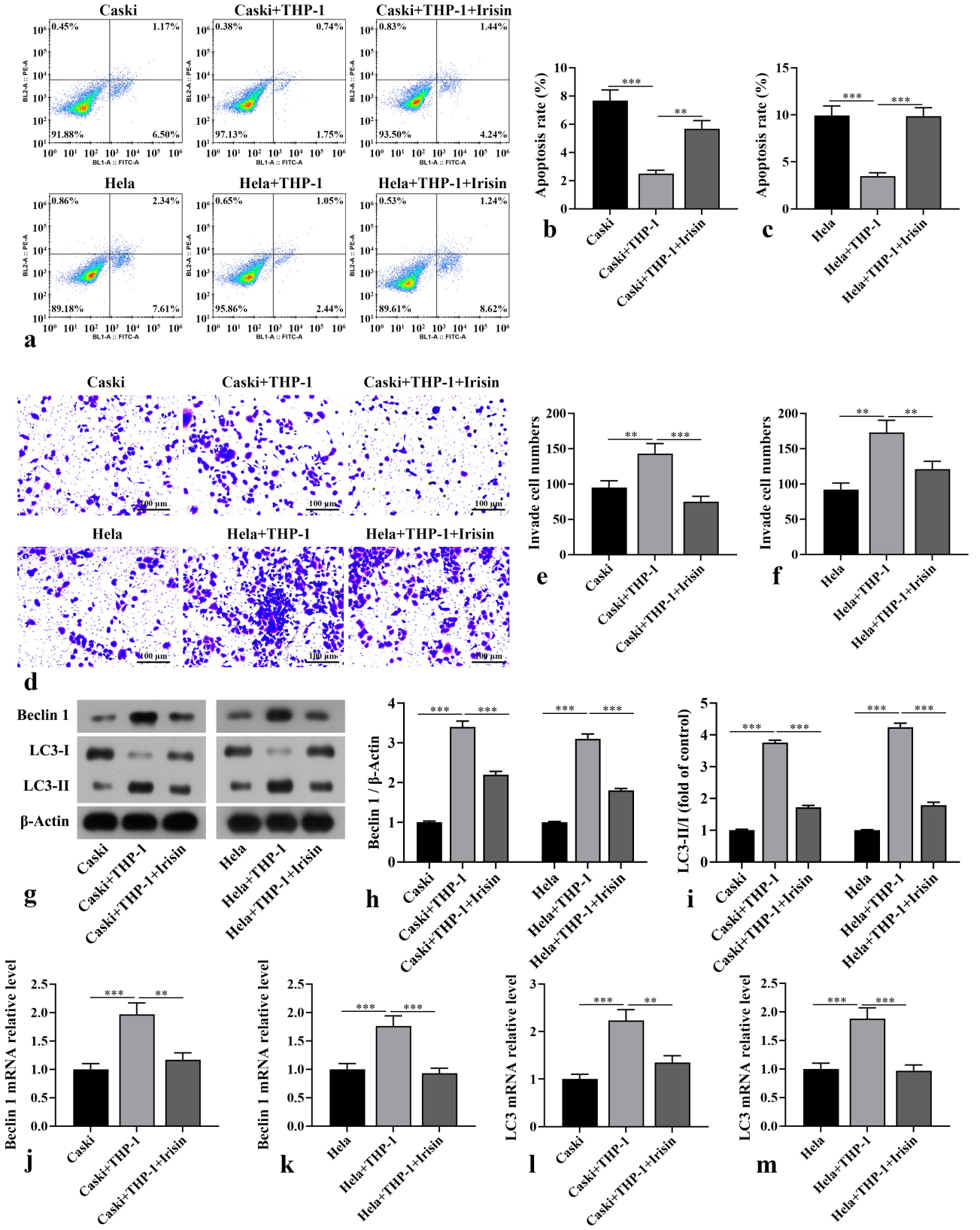

Fig. 5. Irisin modulates the effect of macrophage THP-1 on cervical cancer cell activity. (a–c) Flow cytometry was used to assess apoptosis (n = 3). (d–f) The Transwell assay was used to assess cell invasion (n = 3). (g–i) WB analysis was used to determine autophagy-related markers Beclin 1 and LC3 expression levels (n = 3). (j–m) qRT-PCR was used to assess autophagy-related markers Beclin 1 and LC3 mRNA levels (n = 6). $^{**}p < 0.01$, $^{***}p < 0.001$. qRT-PCR, quantitative real-time polymerase chain reaction.

cells after irisin treatment. This inhibitory effect likely involves multiple mechanisms. We investigated the impact of irisin on cell cycle regulation, as normal cell cycle progression is crucial for proliferation. The findings reveal that irisin causes cell cycle arrest in the G0/G1 phase, significantly reducing the expression of proliferation-associated markers.

Autophagy is an intracellular self-degradation process that helps cells cope with external stress; however, excessive autophagy can provide survival advantages to cancer cells [23]. We found that irisin treatment substantially reduced the expression of autophagy-associated proteins LC3 and Beclin-1 in cervical cancer cells. Simultaneously, the activity of apoptosis-related proteins, particularly caspases, was enhanced. Caspases, a family of cysteine-aspartic acid-specific proteases, play a crucial role in apoptosis [24]. These results suggest that irisin regulates autophagy and apoptosis-related signaling pathways, promoting cells toward apoptosis. To further examine autophagy, we used flow cytometry to assess the apoptosis rate and found that irisin treatment significantly increased the number of apoptotic cells. Metastasis, a hallmark of cancer progression, depends on tumor cell migration and invasion [25]. Using a scratch wound healing assay, we observed that irisin treatment inhibited the wound healing efficiency of cervical cancer cells, thereby reducing their migratory capacity. Since degradation of the extracellular matrix is crucial for cancer cell migration, the effect of irisin may be mediated by downregulating MMPs, which are key enzymes involved in matrix degradation.

Tumor-associated macrophages (TAMs) are key components of TME and play a crucial role in cancer progression [26]. In the TME of cervical cancer, macrophages account for 30%–50% of the cellular composition, highlighting their impact on disease progression [27]. There is a mutual interaction between cancer cells and macrophages. For example, cytokines like IL-6 secreted by cervical cancer cells (HeLa) can promote macrophages toward an M2 phenotype, thereby enhancing tumor proliferation. Moreover, these M2 macrophages, influenced by the local tumor micro-environment, continuously secrete cytokines and growth factors that promote tumor recurrence and significantly increase the likelihood of poor prognosis [28]. Experimental observations revealed that irisin treatment increased the expression of M1-associated markers such as CD86, IL-6, and TNF-α, while decreasing the expression of M2-associated markers, such as IL-10. These observations indicate that irisin can alter macrophage polarization towards an anti-tumor M1 phenotype. We further investigated the impact of this shift and analyzed the effect of macrophage polarization on the biological behavior of cervical cancer cells. Our findings revealed that co-culturing macrophages with cervical cancer cells led to decreased apoptosis rate, increased invasive capacity, and elevated autophagy, all of which promoted tumor progression. As expected, adding irisin to the co-culture reversed these tumor-promoting effects, underscoring its role in inhibiting the development of cervical cancer cells.

Despite its promising results, this study has some limitations. Research on irisin is still in its early stages, and many aspects remain unexplored. For instance, the precise metabolic pathways and mechanisms by which irisin works *in vivo* are not yet fully understood, and its safety and therapeutic efficacy need further clinical investigation. Additionally, the TME is a complex ecosystem consisting of various cell types. However, this study assessed only macrophages and cervical cancer cells, which may cause experimental bias and limit the comprehensiveness of the findings. Future research should validate the findings using animal models to elucidate its therapeutic potential as a novel option in cervical cancer management.

Conclusion

In conclusion, irisin exhibits potent anti-cancer effects on cervical cancer cells by modulating several key cellular processes and altering the TME. Irisin effectively inhibits the proliferation, invasion, and migration of cervical cancer cells and affects the levels of autophagy and apoptosis. Furthermore, it inhibits cancer cells by affecting the polarization of tumor-associated macrophages. The study provides novel insights into the impact of irisin on cervical cancer cells and confirms its potential as a novel therapeutic option.

Availability of Data and Materials

The data used to support the findings of this study are available from the corresponding author upon request.

Author Contributions

GYC and XJM designed the research. GYC and YW performed the research. GYC and YW analyzed the data. All authors were involved in the drafting and critical revision of the manuscript. All authors have read and approved the final manuscript. All authors have participated sufficiently in the work and agreed to be accountable for all aspects of the work.

Ethics Approval and Consent to Participate

Not applicable.

Acknowledgment

Not applicable.

Funding

This research received no external funding.

Conflict of Interest

The authors declare no conflict of interest.

References

[1] Shrestha AD, Neupane D, Vedsted P, Kallestrup P. Cervical Cancer Prevalence, Incidence and Mortality in Low and Middle Income Countries: A Systematic Review. Asian Pacific Journal of Cancer Prevention: APJCP. 2018; 19: 319–324. https://doi.org/10.22034/APJCP.2018.19.2.319.

[2] Sniadecki M, Wydra DG, Wojtylak S, Wycinka E, Liro M, Sniadecka N, *et al*. The impact of low volume lymph node metastases and stage migration after pathologic ultrastaging of non-sentinel lymph nodes in early-stage cervical cancer: a study of 54 patients with 4.2 years of follow up. Ginekologia Polska. 2019; 90: 20–30. https://doi.org/10.5603/GP.2019.0004.

[3] Jiao J, Zhang T, Jiao X, Huang T, Zhao L, Ma D, *et al*. hsa_circ_0000745 promotes cervical cancer by increasing cell proliferation, migration, and invasion. Journal of Cellular Physiology. 2020; 235: 1287–1295. https://doi.org/10.1002/jcp.29045.

[4] Boström P, Wu J, Jedrychowski MP, Korde A, Ye L, Lo JC, *et al*. A PGC1-α-dependent myokine that drives brown-fat-like development of white fat and thermogenesis. Nature. 2012; 481: 463–468. https://doi.org/10.1038/nature10777.

[5] Pinkowska A, Podhorska-Okołów M, Dzięgiel P, Nowińska K. The Role of Irisin in Cancer Disease. Cells. 2021; 10: 1479. https://doi.org/10.3390/cells10061479.

[6] Tsiani E, Tsakiridis N, Kouvelioti R, Jaglanian A, Klentrou P. Current Evidence of the Role of the Myokine Irisin in Cancer. Cancers. 2021; 13: 2628. https://doi.org/10.3390/cancers13112628.

[7] Rabiee F, Lachinani L, Ghaedi S, Nasr-Esfahani MH, Megraw TL, Ghaedi K. New insights into the cellular activities of Fndc5/Irisin and its signaling pathways. Cell & Bioscience. 2020; 10: 51. https://doi.org/10.1186/s13578-020-00413-3.

[8] Celik Z, Baygutalp NK, Kilic AF, Tekin SB, Bakan E, Gul MA, *et al*. Serum irisin levels in colorectal cancer patients. European Review for Medical and Pharmacological Sciences. 2023; 27: 1474–1479. https://doi.org/10.26355/eurrev_202302_31387.

[9] Shi G, Tang N, Qiu J, Zhang D, Huang F, Cheng Y, *et al*. Irisin stimulates cell proliferation and invasion by targeting the PI3K/AKT pathway in human hepatocellular carcinoma. Biochemical and Biophysical Research Communications. 2017; 493: 585–591. https://doi.org/10.1016/j.bbrc.2017.08.148.

[10] Do DV, Park SY, Nguyen GT, Choi DH, Cho EH. The Effects of Irisin on the Interaction between Hepatic Stellate Cell and Macrophage in Liver Fibrosis. Endocrinology and Metabolism (Seoul, Korea). 2022; 37: 620–629. https://doi.org/10.3803/EnM.2022.1412.

[11] Benvenuto M, Focaccetti C. Tumor Microenvironment: Cellular Interaction and Metabolic Adaptations. International Journal of Molecular Sciences. 2024; 25: 3642. https://doi.org/10.3390/ijms25073642.

[12] Bruch-Oms M, Olivera-Salguero R, Mazzolini R, Del Valle-Pérez B, Mayo-González P, Beteta Á, *et al*. Analyzing the role of cancer-associated fibroblast activation on macrophage polarization. Molecular Oncology. 2023; 17: 1492–1513. https://doi.org/10.1002/1878-0261.13454.

[13] Cortés-Morales VA, Chávez-Sánchez L, Rocha-Zavaleta L, Espíndola-Garibay S, Monroy-García A, Castro-Manrreza ME, *et al*. Mesenchymal Stem/Stromal Cells Derived from Cervical Cancer Promote M2 Macrophage Polarization. Cells. 2023; 12: 1047. https://doi.org/10.3390/cells12071047.

[14] Guo F, Kong W, Li D, Zhao G, Anwar M, Xia F, *et al*. M2-type tumor-associated macrophages upregulated PD-L1 expression in cervical cancer via the PI3K/AKT pathway. European Journal of Medical Research. 2024; 29: 357. https://doi.org/10.1186/s40001-024-01897-2.

[15] Salmaninejad A, Layeghi SM, Falakian Z, Golestani S, Kobravi S, Talebi S, *et al*. An update to experimental and clinical aspects of tumor-associated macrophages in cancer development: hopes and pitfalls. Clinical and Experimental Medicine. 2024; 24: 156. https://doi.org/10.1007/s10238-024-01417-w.

[16] Kerneur C, Cano CE, Olive D. Major pathways involved in macrophage polarization in cancer. Frontiers in Immunology. 2022; 13: 1026954. https://doi.org/10.3389/fimmu.2022.1026954.

[17] Xu F, Cui WQ, Wei Y, Cui J, Qiu J, Hu LL, *et al*. Astragaloside IV inhibits lung cancer progression and metastasis by modulating macrophage polarization through AMPK signaling. Journal of Experimental & Clinical Cancer Research: CR. 2018; 37: 207. https://doi.org/10.1186/s13046-018-0878-0.

[18] Symonds EKC, Black B, Brown A, Meredith I, Currie MJ, Hally KE, *et al*. Adipose derived stem cell extracellular vesicles modulate primary human macrophages to an anti-inflammatory phenotype in vitro. Journal of Extracellular Biology. 2023; 2: e104. https://doi.org/10.1002/jex2.104.

[19] Pinto SM, Kim H, Subbannayya Y, Giambelluca MS, Bösl K, Ryan L, *et al*. Comparative Proteomic Analysis Reveals Varying Impact on Immune Responses in Phorbol 12-Myristate-13-Acetate-Mediated THP-1 Monocyte-to-Macrophage Differentiation. Frontiers in Immunology. 2021; 12: 679458. https://doi.org/10.3389/fimmu.2021.679458.

[20] Tekin S, Erden Y, Sandal S, Yilmaz B. Is Irisin an Anticarcinogenic Peptide? Medicine Science. 2015; 4: 2172–2180. https://doi.org/10.5455/medscience.2014.03.8210.

[21] Gopu P, Antony F, Cyriac S, Karakasis K, Oza AM. Updates on systemic therapy for cervical cancer. The Indian Journal of Medical Research. 2021; 154: 293–302. https://doi.org/10.4103/ijmr.IJMR_4454_20.

[22] Cebulski K, Nowińska K, Jablońska K, Romanowicz H, Smolarz B, Dzięgiel P, *et al*. Expression of Irisin/FNDC5 in Breast Cancer. International Journal of Molecular Sciences. 2022; 23: 3530. https://doi.org/10.3390/ijms23073530.

[23] Huang H, Han Q, Zheng H, Liu M, Shi S, Zhang T, *et al*. MAP4K4 mediates the SOX6-induced autophagy and reduces the chemosensitivity of cervical cancer. Cell Death & Disease. 2021; 13: 13. https://doi.org/10.1038/s41419-021-04474-1.

[24] Kesavardhana S, Malireddi RKS, Kanneganti TD. Caspases in Cell Death, Inflammation, and Pyroptosis. Annual Review of Immunology. 2020; 38: 567–595. https://doi.org/10.1146/annurev-immunol-073119-095439.

[25] Liu H, Ye X, Li D, Yao Q, Li Y. Incidence, clinical risk and prognostic factors for liver metastasis in patients with cervical cancer: a population-based retrospective study. BMC Cancer. 2021; 21: 421. https://doi.org/10.1186/s12885-021-08127-6.

[26] Bahri M, Anstee JE, Opzoomer JW, Arnold JN. Perivascular tumor-associated macrophages and their role in cancer progression. Essays in Biochemistry. 2023; 67: 919–928. https://doi.org/10.1042/EBC20220242.

[27] Guo W, Liu W, Wang J, Fan X. Extracellular vesicles and macrophages in tumor microenvironment: Impact on cervical cancer. Heliyon. 2024; 10: e35063. https://doi.org/10.1016/j.heliyon.2024.e35063.

[28] Yan X, Zhang S, Jia J, Yang J, Song Y, Duan H. Exosomal MiR-423-3p inhibits macrophage M2 polarization to suppress the malignant progression of cervical cancer. Pathology, Research and Practice. 2022; 235: 153882. https://doi.org/10.1016/j.prp.2022.153882.